JOURNAL OF MATERIALS SCIENCE **40** (2005) 5223–5232

Study of conduction mechanism in aluminium and magnesium co-substituted lithium ferrite

M. P. PANDYA, K. B. MODI, H. H. JOSHI
Department of Physics, Saurashtra University, Rajkot-360005, India
E-mail: kunalbmodi2003@yahoo.com

The conduction mechanism in Mg^{2+} and Al^{3+} substituted $Li_{0.5}Fe_{2.5}O_4$ with general formula $Mg_xAl_{2x}Li_{0.5(1-x)}Fe_{2.5(1-x)}O_4$ ($x = 0.0$, 0.2, 0.5, 0.6 and 0.7) has been studied by means of compositional and temperature dependent d.c. resistivity, thermoelectric power and I–V characteristics measurements. It is found that ferrites are electronic conductors. For $x = 0.0$ and 0.2 conduction is due to holes, while for $x = 0.5$, 0.6 and 0.7 it is due to electrons. Thermal variation of mobilities and activation energies determined through d.c. resistivity measurements confirm the formation of small polarons. The sample with $x = 0.0$ exhibits switching phenomena.

1. Introduction

The field of ferrites is very old but due to their various potential applications and interesting physics involved in it, even after more than half a century, scientists, researchers and engineers are still interested in various types of ferrite materials, substituted with different cations, prepared by different techniques and its various properties as a function of compositions, temperature, frequency etc. The study of electric and dielectric behaviour carry equal importance, as magnetic properties from both applied and fundamental research points of view. The electrical properties such as d.c. resistivity, thermoelectric power, I–V characteristics provide vital information regarding activation energy, type of charge carriers responsible for conduction mechanism, carrier concentration, its mobility and related aspects. To our knowledge only few reports are available in literature on various electrical properties of substituted lithium ferrites [1–6]. The aim of the present work is to study the conduction mechanism in magnesium and aluminium co-substituted lithium ferrites, which is in continuation to our earlier study on magnetic [7] and structural properties [8] of the $Mg_xAl_{2x}Li_{0.5(1-x)}Fe_{2.5(1-x)}O_4$ system.

2. Experimental procedure

The powdered samples of $Mg_xAl_{2x}Li_{0.5(1-x)}Fe_{2.5(1-x)}O_4$ have been prepared by the usual double sintering ceramic method, with compositions $x = 0.0$, 0.2, 0.5, 0.6 and 0.7. The details regarding sample preparation and X-ray diffractometry have been given in our earlier communications [7, 8].

The samples for electrical measurements were in the form of disc 10 mm in diameter and 3 mm thick. Both faces of each disc sample were polished by rubbing with zero grade emery paper, washed in dilute HCl and acetone. Finally, graphite was rubbed on both flat faces of the samples on which aluminium foil was also kept for good electrical contacts. The resistance of a pellet was measured by the two terminal pressure contact method using a BPL Meg-ohm meter. Thermal variation of resistance was obtained by placing sample holder containing a pellet in a horizontal electric furnace; temperature was measured by a chromel-alumel thermo-couple. The resistance of the pellet was measured during the decrease of temperature at steps of 20°C.

Thermoelectric power studies were carried out over a temperature range 300–550 K by the differential method. The temperature gradient was measured by two chromel-alumel thermo-couples which were kept very close to the sample while the thermo-emf was measured with the help of a digital microvoltmeter with an accuracy of ±3%. In order to achieve good thermal stability, the values of the thermo-emf have been recorded while cooling. The sample is maintained at a given temperature for about 5–10 min.

Current versus voltage measurements were performed in the voltage range of 0–500 V using an Aplab high voltage d.c. regulated power supply (model: 7332). The measurements were carried out for two different temperatures of 300 and 450 K.

3. Results and discussion

For precise electrical measurements such as resistivity and thermoelectric power, ohmic contact is the first stringent requirement [9]. To ascertain the ohmic contact between pellet and electrode interface the current through each pellet was measured as a function of applied d.c. voltage at constant temperature and the results were plotted as J (current density) against E (applied electric field). Typical plots for compositions $x = 0.2$, 0.6 and 0.7 are shown in Fig. 1. Reversal of the electric

0022–2461
DOI: 10.1007/s10853-005-4416-z

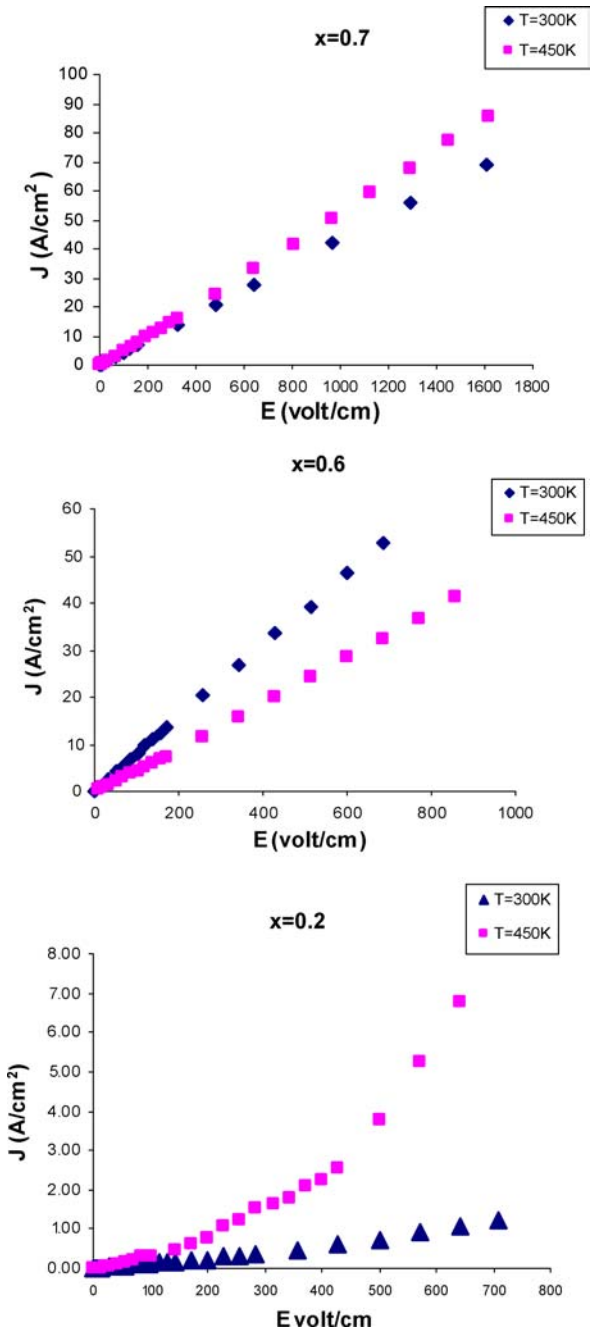

Figure 1 Variation of electric current density J with applied electric field E for $x = 0.2$, 0.6 and 0.7.

field does not have any effect on these measurements. It is seen that the J–E plots are linear in the applied electric field range from 1 to 400 V/cm, indicating the presence of ohmic contacts at the pellet-electrode interface in the temperature range of the measurements. Of course, for $x = 0.0$ and 0.2 the deviation from linearity has been observed for $E > 400$ V/cm, and indicating non-ohmic contact. Therefore, the electric field strengths which guarantee ohmic contact were used.

The compositional dependence of resistivity ($\log_{10}\rho$) at 363 K is represented in Table II. It was observed from Table I that the highest observed value of bulk density (d) remains less than the X-ray density (d_x) of the material. This indicates that even highly pressed and sintered pellets contain pores. Therefore, a correction for pore fraction has to be applied to obtain the crystalline value

TABLE I Lattice constant (a), X-ray density (dx), bulk density (d) and pore fraction (f) for Mg-Al-Fe-Li-O system

Content x	Lattice constant a (Å) ± 0.002 Å	dx (g/cm^3)	d (g/cm^3) $P = 2 \times 10^7$kg/m^2	f
0.0	8.370	4.69	4.10	0.125
0.2	8.332	4.49	3.96	0.116
0.5	8.275	4.09	3.47	0.151
0.6	8.281	4.02	3.36	0.165
0.7	8.234	3.87	3.19	0.175

of electrical resistivity. This has been done using the relation [10]:

$$\rho = \rho_p[1 + f(1 + f^{\frac{2}{3}})^{-1}]^{-1} \quad (1)$$

where ρ is corrected value, ρ_p is measured value of d.c. resistivity and f is pore fraction (Table I). Equation 1 seems to hold good for $f < 0.4$. The resistivity, in general, increases with increase in Mg-Al content (x). This happens because the replacement of Fe^{3+} by Mg^{2+} and Al^{3+} in $Mg_xAl_{2x}Li_{0.5(1-x)}Fe_{2.5(1-x)}O_4$ system reduces conduction through the octahedral sites. The incorporation of Mg-Al ions which do not participate in the conduction process, limits the degree of $Fe^{3+} + Fe^{3+} \leftrightarrow Fe^{4+} + Fe^{2+}$ conduction that occurs. Thus, the efficient method of curtailing the conduction process is the replacement of the effective ion (Fe^{3+}) by less effective ones (Mg^{2+} and Al^{3+}).

We have co-related jump length (L) of the charge carriers between Fe^{3+} and Fe^{2+} ions (for n-type conduction; $x = 0.5$, 0.6 and 0.7) and Fe^{4+} and Fe^{3+} (for p-type conduction; $x = 0.0$, 0.2) on the octahedral site to the electrical resistivity. The jump length (L) is determined from the relation [11]

$$L = a\sqrt{2}/4$$

where a is the lattice constant (Table I). The values of jump length L for various values of Mg-Al content (x) is summarized in Table II. This shows that L decreases with increasing content (x). This is due to the fact that on substitution of Mg-Al in the system $Mg_xAl_{2x}Li_{0.5(1-x)}Fe_{2.5(1-x)}O_4$, Al^{3+} with smaller ionic radius (0.51 Å) preferentially occupy the octahedral B-site, by replacing larger Li^{1+} (0.70 Å) and Fe^{3+} (0.64 Å) ions. The replacement of larger cations by smaller one, results in a decrease in B-site ionic radius from 0.655 Å ($x = 0.0$) to 0.560 Å ($x = 0.7$) [6] causing the jump length L to decrease with increasing concentration (x). The observed decrease in L with x suggests that charge carriers require less energy to jump from one cationic site to other which causes a decrease in resistivity with increaseing x. The present results on the variation of d.c. resistivity with x show that ρ_{dc} increases with increasing x (Table II). This discrepancy can be explained as follows: In the present system, due to the substitution of Al^{3+}, site ionic radius and therefore, the jump length decreases, but at the same time Fe^{3+} ion concentration and its B-site occupancy also decreases [5, 6]. The decrease in Fe^{3+} concentration on B-sites, reduces the Fe^{3+}/Fe^{2+}- and

TABLE II Resistivity ($\log_{10}\rho$), jump length (L), activation energy (E), Fermi energy ($E_F(o)$), polaron radius (r_p)

Content (x)	$\log_{10}\rho$ ($\Omega\cdot$cm) (363 K)	Jump length L (Å)	Acticvation energy (eV) E_p	E_f	$\Delta E = E_p - E_f$ (eV)	Fermi energy $E_F(o)$ (eV)	Polaron radius r_p	η_i	K_i
0.0	5.22	2.96	0.792	0.385	0.407	–	0.737	0.56	−176.05
0.2	5.72	2.94	0.496	0.396	0.198	0.06	0.733	−0.46	533.18
0.5	8.61	2.93	0.594	0.372	0.222	0.86	0.728	−7.99	3434.02
0.6	10.25	2.93	0.880	0.594	0.286	2.40	0.729	−16.49	8500.70
0.7	8.60	2.91	0.448	–	0.448	0.25	0.725	−5.59	2354.23

Fe^{3+}/Fe^{4+}-ratios responsible for the conduction process in the ferrites. Thus, the resistivity increases with increasing x (Table II).

The thermoelectric power or Seebeck coefficient (α) does not show any pressure dependence within the accuracy of our measurement and does not warrant correction for pore fraction. Even after correcting for pore fraction, it is essential to see how significant the grain-boundary effects are. To see this, ρ_{ac} was measured as a function of applied signal frequency at constant temperatures for all the ferrites and typical plots for all the compositions are shown in Fig. 2. It has been observed that there is only slight variation of ρ_{ac} at lower temperature, however it remains independent of frequency at higher temperature ($T > 550$ K). This indicates that grain-boundary effects are sufficiently minimized for highly pressed pellets at least at higher temperatures.

The first step in the understanding of electrical transport in any solid is to know whether conductivity is ionic, electronic or mixed (partially ionic and electronic). There are several ways of determining this [12]. One of the ways is to study the d.c. resistivity (ρ_{dc}) and the a.c. resistivity (ρ_{ac}) as a function of temperature. If ρ_{ac} is larger than ρ_{dc} this suggests dielectric behaviour emanating from ionic conductivity. If $\rho_{ac} = \rho_{dc}$, it indicates predominance of electronic conduction. For the sake of comparison, the variation of a.c. resistivity (1 kHz) with temperature was carried out for typical composition $x = 0.2$, see Fig. 3a. It is seen that for the entire temperature range, ρ_{ac} coincides with ρ_{dc}, suggesting electronic conduction [13].

It is known that in the case of pure ionic conduction, ρ_{dc} increases with time and tends to become infinite after a sufficiently long time; whereas for a pure electronic conductor it is essentially independent of time. For mixed conduction it increases with time but tends to stabilize at some finite value, which is the electronic contribution [14]. Therefore, ρ_{dc} for all the compositions was measured at constant temperature ($T = 363$ K) as a function of time using platinum foil electrodes [15], which blocks ionic conduction. The typical results for $x = 0.2$, 0.5, and 0.7 are shown in Fig. 3b. It was observed that ρ_{dc} increases with time but becomes almost constant after 30 seconds. The ratio of instantaneous $\rho_{dc}(0)$, to steady state, $\rho_{dc}(\infty)$ electrical resistivity varies from 0.92 to 0.95 for different ferrites at different temperatures. This indicates that the synthesized ferrite samples are essentially electronic conductors and ionic conduction remains less than 9% at all temperatures.

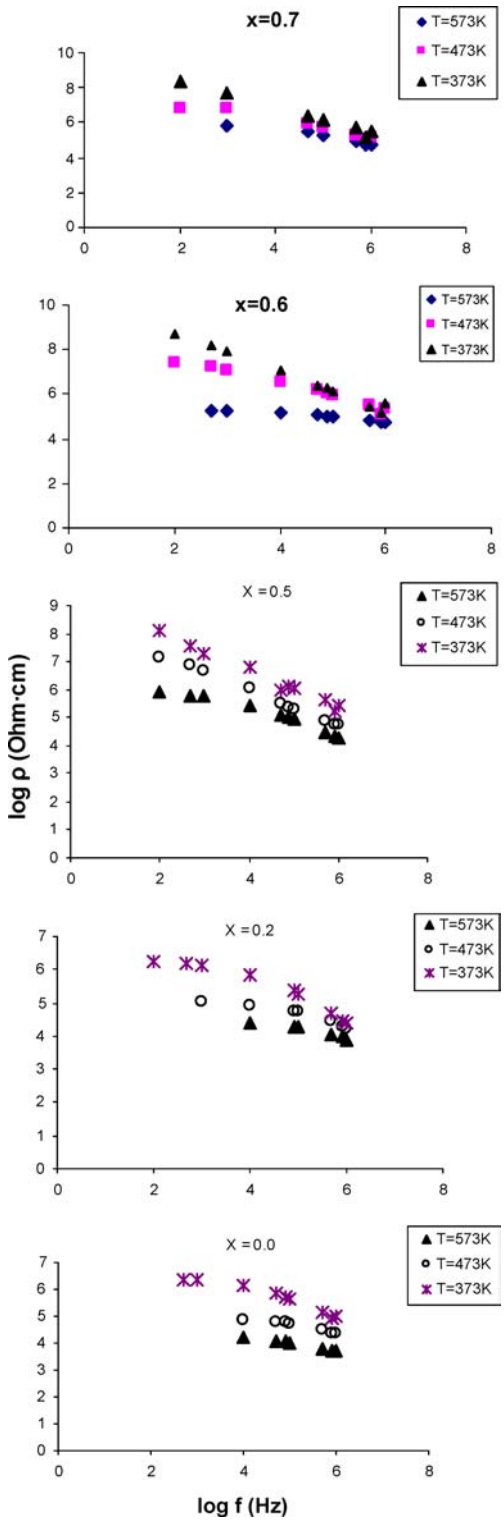

Figure 2 Pellet electrical resistivity versus applied signal frequency ($\log f$) for $x = 0.0$, 0.2, 0.5, 0.6, and 0.7 at constant temperature.

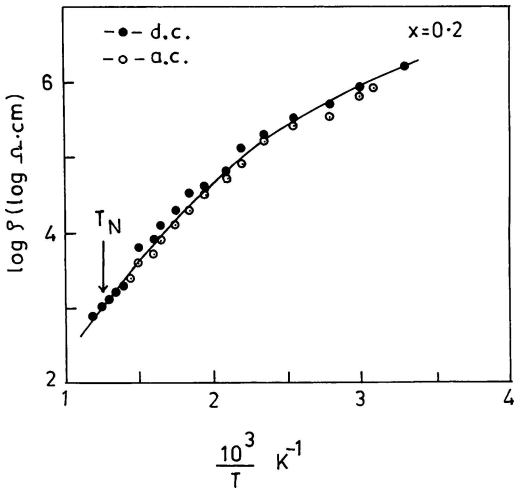

(a)

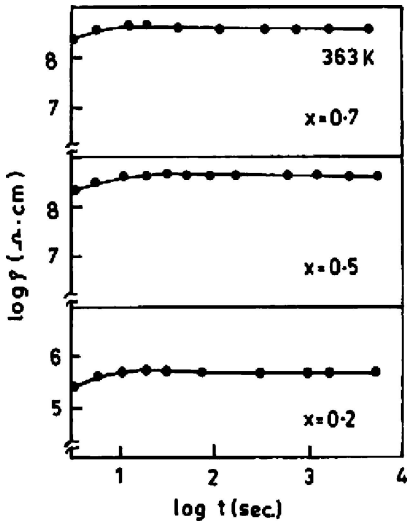

(b)

Figure 3 (a) Electrical resistivity versus temperature for $x = 0.2$. (b) Electrical resistivity as a function of time at 363 K for $x = 0.2$, 0.5, and 0.7.

3.1. Thermal variation of d.c. resistivity measurements

The d.c. electrical resistivity of pellets of each ferrite made at pressure $(P) \approx 2 \times 10^7$ kg/m^2 and sintered at 1150°C for 24 h have been measured as a function of temperature (300–1000 K). The resistivity values for a particular ferrite do not differ much from sample to sample. Furthermore, for each pellet no significant difference has been observed in resistivity values during the heating and cooling cycles. The ρ_{dc} values for a series of ferrites lie between 10^5–10^{10} $\Omega \cdot$ cm near room temperature (Table II), obviously they will be good insulators at room temperature. The ρ_{dc} variation with temperature for compositions $x = 0.0$, 0.2, 0.5, 0.6, and 0.7 are presented in Fig. 4 as plots of $\log_{10}\rho$ gainst $10^3/T$. It is interesting to note that the nature of the curve for compositions $x = 0.0$ and 0.2 is different from that for $x = 0.5$, 0.6 and 0.7. For the former ferrites the $\log\rho$ versus reciprocal of temperature curve consist of three distinct regions and two breaks, while $x = 0.5$ and 0.6 show two slopes with a single transition. For $x = 0.7$ no break is observed. The temperature T_1 corresponds to the transition from region I to II and temperature

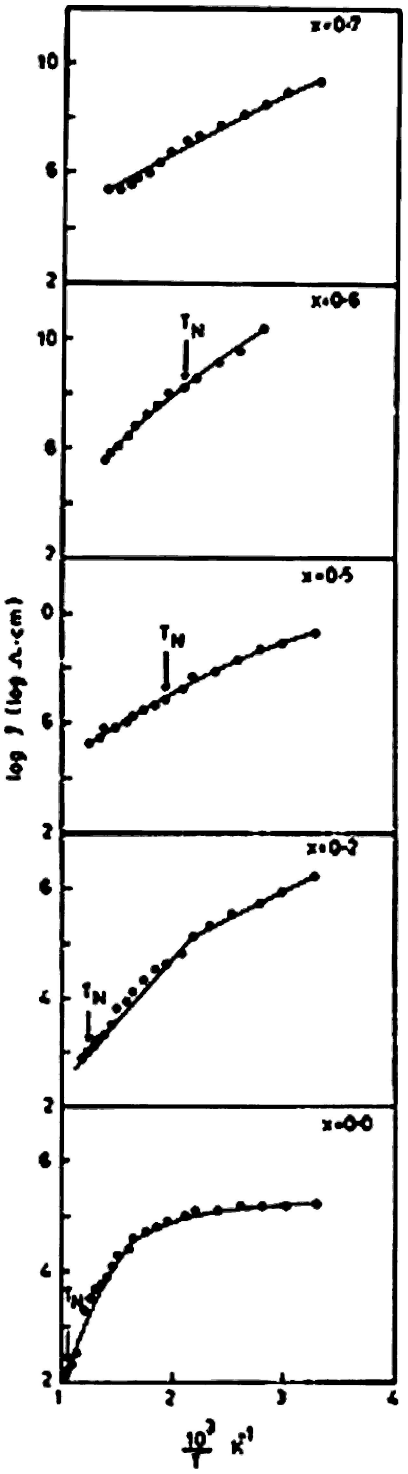

Figure 4 Electrical resistivity (ρ_{dc}) versus temperature for $x = 0.0$, 0.2, 0.5, 0.6, and 0.7.

T_2 from region II to III. Similar type of behaviour has been observed for Li–Cu ferrite [16], Zr^{4+} substituted Cu-ferrite [17], and Mn^{2+} and Ti^{4+} substituted Ni–Zn ferrite [18]. The transition temperature, T_2 ($x = 0.0$ and 0.2) and T_1 ($x = 0.5$, 0.6 and 0.7), is close to the Neel temperature of the ferrites. Ghani *et al.* [19] observed three regions in the temperature variation of resistivity for Cu–Ni ferrites. They attributed the conduction mechanism in the first region to the presence of impurities, in the second region to the phase transition, and in the third region to magnetic disorder. The conduction process in the present material may be due to

TABLE III Neel temperature (T_N) for Mg-Al-Li-Fe-O system

	Neel temperature (K)			
Content (x)	Susceptibility	Theoretical	Resistivity	Mobility
0.0	970	970	952	–
0.2	803	787	800	–
0.5	512	502	513	–
0.6	410	403	476	435
0.7	–	303	–	392

grains, grain structure and porosity in region-I, order of Li ions, crystal structure changes in region-II and magnetic disorder in region III. The Neel temperature (T_N) deduced for the compositions with $x = 0.0$, 0.2, 0.5, and 0.6 from $\log\rho$ versus $10^3/T$ plots are listed in Table III. It is found that the values of T_N are in good agreement to those found experimentally from a.c. susceptibility measurements [5] and theoretically by applying molecular field theory (Table III). The absence of a slope change or transition for $x = 0.7$ may be due to the fact that its Neel temperature is close to room temperature (≈303 K; Table III).

The Seebeck coefficient measurements on the present system $Mg_xAl_{2x}Li_{0.5(1-x)}Fe_{2.5(1-x)}O_4$ have established that all the samples except those with $x = 0.0$ and 0.2 are n-type semiconductors. This indicates that the most probable conduction mechanism is electron hopping between Fe^{2+} and Fe^{3+} ions

$$Fe^{2+} \leftrightarrow Fe^{3+} + e^- \quad \text{(n-type)}$$

This process is expected to take place between two adjacent octahedral sites in the spinel lattice.

As shown in Fig. 4, the plot consists of two straight line portions; hence there are two activation energies for the two different regions. The reason for the two slopes can be explained as follows: At high temperature, the thermal energy is sufficiently great to create vacancies and the activation energies represent a sum of the energies required for vacancies generation and the motion of electrons into the vacancies. At lower temperature, the thermal energy is only large enough to allow the migration of electrons into vacancies already present in the crystal. A change in the slope may be due to the Neel temperature [20] or to the change in the conductivity mechanism [21]. This anomaly strongly supports the influence of magnetic ordering upon the conduction process.

The temperature dependence of resistivity is given by the Arrhenius equation

$$\rho = \rho_o \exp(\Delta E/kT) \qquad (2)$$

where k is Boltzman constant, ΔE is the activation energy and T is the absolute temperature.

The activation energies for conduction are computed from $\log_{10}\rho$ versus $10^3/T$ plots and are presented in Table II. The activation energy increases on changing from ferrimagnetic (E_f) to paramagnetic (E_p) region. According to the theory of magnetic semiconductors, one expects such a reduction in the activation energy as the system undergoes the transition from the paramagnetic to the ferrimagnetic state. This is due to fact that the ferrimagnetic state is an ordered state while the paramagnetic state is disordered, thus charge carriers required more energy for the conduction. The high value of the activation energy in the paramagnetic state as compared to ferrimagnetic state is due to the volume expansion of the samples during the magnetic transition [22, 23]. The activation energies in the ferrimagnetic region are much higher than the ionization energies ($E_i = 0.1$ eV) of donor or acceptors and hence the possibility of band type conduction is ruled out. These values are also higher than the transition energy of Fe^{2+} and Fe^{3+} ($E_e = 0.2$ eV), which indicate that the polaron type conduction mechanism is favoured.

In ferrites, cations are surrounded by close packed oxygen anions and, as a first approximation, can well be treated as isolated from each other. There will be little direct overlap of the anion charge clouds or orbitals. Alternatively, the electrons associated with particular ions will largely remain isolated and, hence, a localized electron model is more appropriate in the case of ferrites rather than the collective electron (band) model. In ferrites, the charge carriers are not completely free but are strongly localized in the d-shell; this localization may be due to the electron-phonon interaction (or formation of polarons). A small polaron defect is created when an electronic carrier becomes trapped at a given site as a consequence of the displacement of adjacent atoms or ions. The entire defect (carrier plus distortion) then migrates by an activated hopping mechanism. The small polaron model also explains the low value of mobility, temperature independent Seebeck coefficient and thermally activated hopping. An essential conditions for the formation of a small polaron is that the value of polaron radius (r_p) should be less than the inter ionic distances. An attempt has been made to calculate the polaron radius for all the compositions studied by the relation [24].

$$r_p = \frac{1}{2}\left[\frac{\pi}{6N}\right]^{\frac{1}{3}}$$

where N = Number of sites per unit volume = $96/a^3$.

In spinel ferrites 64 A (tetrahedral) and 32 B (octahedral) sites are available per unit volume. The calculated values of r_p for $x = 0.0, 0.2, 0.5, 0.6$ and 0.7 are summarized in Table II. It is seen that these values are smaller than inter ionic distances [6], and hence are appropriate for small polaron conduction. Furthermore, in the large polaron model, the resistivity is by band conduction at all temperatures and the a.c. resistivity increases with frequency. The small polarons conduct in band-like manner up to a certain temperature, the resistivity showing a decrease with frequency. At higher temperatures, the conduction is by thermally activated hopping [25–27]. From Fig. 2 it is clear that ρ_{ac} decreases with increasing frequency, giving indirect support for small polaron conduction involving a band-like mechanism. Another important indirect confirmation of small polaron formation, is that the Seebeck coefficient (α) is almost independent of temperature for $T > 340$ K (Fig. 5).

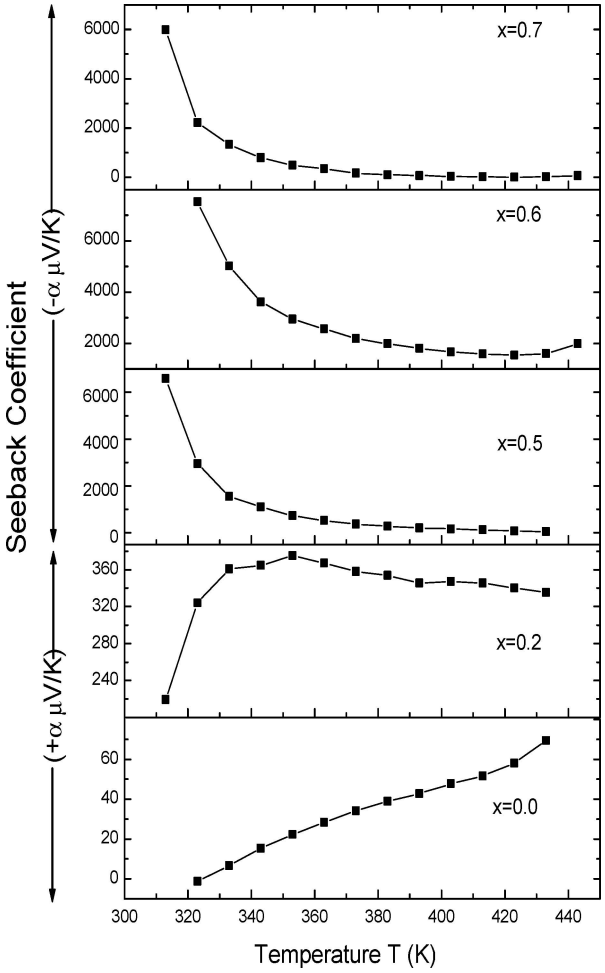

Figure 5 Thermal variation of Seebeck coefficient for $x = 0.0$, 0.2, 0.5, 0.6, and 0.7.

Based on the small polaron model the conduction phenomenon in region I is attributed to the presence of impurities, vacancies and defects, while that at higher temperatures it is attributed to the small polaron hopping mechanism. According to Rezlescu *et al.* [28] the change $\Delta E = E_p - E_f$ (Table II) is associated with the ordering temperature roughly given by the relation $\Delta E = AkT_N$, where E_p and E_f are activation energies below and above T_N. The average value of the proportionality constant 'A' is found to be ~5.1. The value 5.1 is in good agreement with that reported for Cu–Mn–Zn ferrites [28], Cu–Zn–Fe, Cr–O ferrites [29], and Li–Cu ferrites [16].

It is important to note that small changes in ΔE with x are observed for present system (Table II). According to Ahmed *et al.* [30], the effect of x on ΔE is greater if the substituted cations occupy B-sites. Devale *et al.* [31] suggest that almost no change in ΔE is observed when the substitution is made on A-sites without disturbing the B-sites. The small change in ΔE with x for the present system suggest that Mg^{2+} and Al^{3+} ions occupy both cation sites as confirmed by the cation distribution according to [5, 6].

3.2. Thermoelectric power measurements

As mentioned earlier, the thermoelectric power α is positive for the samples with $x = 0.0$ and 0.2, indicating that the majority charge carriers are holes. Thus the conduction mechanism for the p-type semiconductor is due to the hole transfer from Fe^{4+} centers to neighbouring Fe^{3+} ions [32] at the octahedral sites. The thermoelectric voltage (ΔE) developed across each pellet of the ferrite material does not significantly depend upon heating and cooling cycles and reproducible values (within $\pm 10\%$) are obtained in successive observations. The Seebeck coefficient $= \Delta E/\Delta T$ ($\Delta T =$ the temperature difference across the sample) at different temperatures (300–500 K) for the samples studied is shown in Fig. 5. The striking features of the system studied are that (i) α is positive for $x = 0.0$ and 0.2 while it is negative for $x = 0.5$, 0.6 and 0.7 over the whole range of temperature. (ii) α increases with temperature for $x = 0.0$. For $x = 0.2$, it increases up to 360 K and then remains almost constant, while it decreases with increasing temperature for compositions $x = 0.5$, 0.6 and 0.7.

The first observation suggests that for $x = 0.0$ and 0.2, majority charge carriers are holes or p-type conduction is dominant while for $x = 0.5$, 0.6 and 0.7 majority charge carriers are electrons or n-type conduction is dominant. The second observation leads to conclusion that for $x = 0.0$ and 0.2, on increasing temperature the number of Fe^{4+} centers increases, and for $x = 0.2$ above $T > 360$ K it remains constant over the entire temperature range. In the case of $x = 0.5$, 0.6 and 0.7, the decrease in the Seebeck coefficient α with increasing temperature suggest that on increasing temperature the formation of Fe^{3+} to Fe^{4+} is more probable as compared to Fe^{3+} to Fe^{2+}. This decreases the available Fe^{3+}/Fe^{2+} ions responsible for Fe^{3+}–Fe^{2+} exchange.

The positive α values for the $Li_{0.5}Fe_{2.5}O_4$ ($x = 0.0$) ferrite sample increase on increasing temperature for the entire range of temperatures studied. In contrast, for $x = 0.2$ it increases up to ≈353 K . It is due to the thermal enhancement of drift mobility and thermal liberation of excess holes. The decreasing negative values for samples with $x = 0.5$, 0.6, and 0.7 may be due to the recombination of some holes and electrons since both electrons and holes are responsible for electric conduction in these samples. The increase of α for $x = 0.0$ is smaller than the decrease occuring for other samples. This may be due to the fact that the activation energy for electron hopping is less than that for hole hopping [33] and that the drift mobility of electrons (10^{-4} cm^2/volt·sec) is higher than that of the holes (10^{-8} cm^2/volt sec).

Bashikiriv and Liberman [34] have classified ferrites as degenerate semiconductors if the thermo emf is independent of temperature and as non-degenerate semiconductors if the thermo emf depends on temperature. In the present study, sample $x = 0.0$ is a completely non-degenerate semiconductor while samples with $x = 0.2$, 0.5, 0.6, and 0.7 are non-degenerate semiconductors at lower temperatures (<360 K) while they become degenerate for higher temperatures studied (Fig. 5).

In the region where conduction is due to one kind of charge carriers (electrons or holes; not both) the relations between the Seebeck coefficient (α) and Fermi energy (E_F) will be given by [35, 36]

$$E_F = e\alpha T - AkT$$

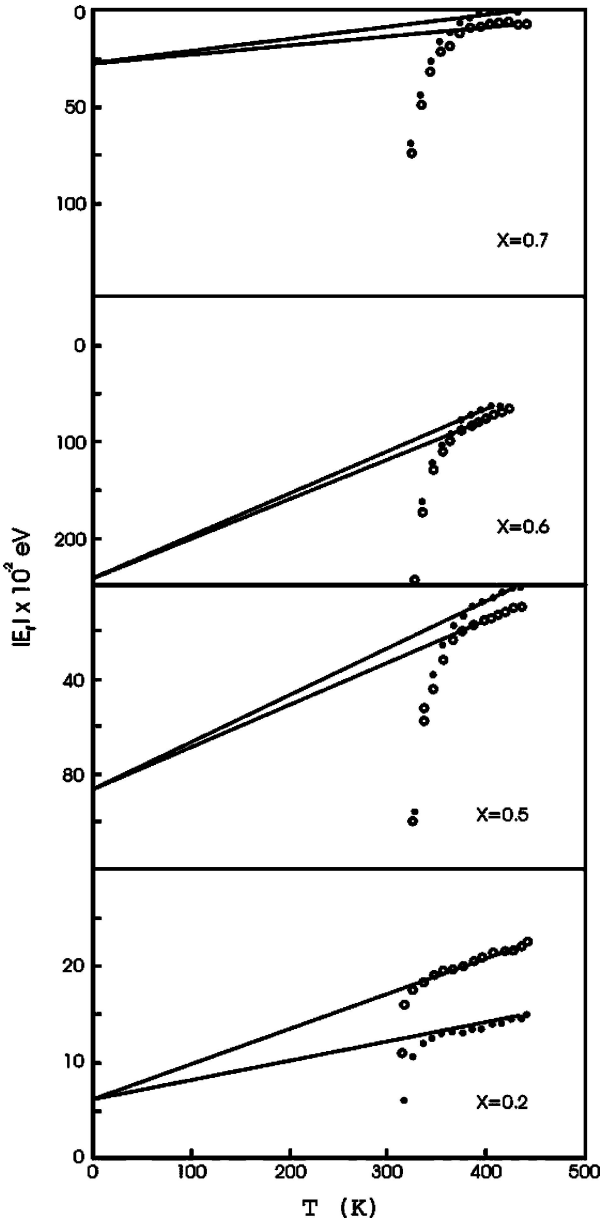

Figure 6 Temperature dependence of Fermi energy (E_f) for $x = 0.2$, 0.5, 0.6, and 0.7.

where A is a term connected with the kinetic energy of charge carriers, e, k and T are charge of carrier; Boltzmann constant (8.6×10^{-5} eV) and absolute temperature, respectively. The calculated values of E_F as a function of temperature for two values of A ($A = 0$ and 2) are shown in Fig. 6. The extrapolated value of E_F to $T = 0$ K, yields the values of E_F (0) (Table II).

Comparing the activation energies of the ferrimagnetic region (E_f) with $E_F(0)$, it is seen that $E_f > E_F(0)$. The difference between the two values can be attributed to the activation energy associated with hopping of charge carriers. Thus, activation energy consists of two components, one that is associated with generation of charge carriers (holes/electrons) and the other associated with the hopping of the carriers between crystallographically equivalent sites.

Within the experimental accuracy the variation of α with temperature (T) can be represented by the following equation:

$$\alpha = \eta_i T^{-1} + K_i$$

where, η_i is the slope and K_i is the intercept of the curve with the α axis (i.e., Y-axis). The summarized results are given in Table II.

3.3. Temperature variation of charge carrier concentration

For a hopping mechanism, the Seebeck coefficient, α is independent of temperature and its magnitude primarily depends upon the density of the charge carriers. It is expressed in the form of the Heikes formula [37],

$$\alpha = \frac{k}{e}\left(\frac{S_r^*}{k} - \log_e \frac{c}{1-c}\right)$$

where S_r^* is the effective entropy of the lattice which is temperature independent and S_r^*/k is very small. c is given by n_c/N, where n_c is the number of carriers in the states and N is the total number of available states. Neglecting the term S_r^*/k from the relation gives

$$\alpha = \frac{k}{e}\log_e\left(\frac{1}{c} - 1\right)$$

If V is the volume of the sample under study above equation can be written as:

$$nc = \frac{N}{V}\left[\frac{1}{1 + \exp\left(\frac{\alpha e}{k}\right)}\right]$$

The values of charge carrier concentration per unit volume have been calculated for all the compositions at each temperature by using the values of the Seebeck coefficient. N is the density of states, in the case of low mobility semiconductors like ferrites having exceedingly narrow bands or localized levels, the value of N can be taken as $10^{22}/\text{cm}^3$ [38, 39]. The plots $\ln(n_c)$ versus $10^3/T$ for various mixed ferrites are shown in Fig. 7. It can be seen from the figures that the carrier concentration behaves inversely as compared to the variation of Seebeck coefficient with temperature. Here, it should to be noted that for the determination of n_c, only $|\alpha|$ should be taken into consideration, because positive and negative signs just indicate whether charge carriers are holes or electrons, it has nothing to do with its value. It is seen from Fig. 7 that for $x = 0.0$ n_c decreases continuously with temperature, for $x = 0.2$ it decreases up to the temperature of ≈353 K and then start increasing. For compositions with $x = 0.5$, 0.6 and 0.7 charge carrier concentration per unit volume increases with increasing temperature. The observed variation of charge carrier concentration (n_c) with temperature for all the compositions can be explain on the following basis:

On increasing temperatures holes which are the majority charge carriers for $x = 0.0$ and 0.2 are compensated by thermally generated electron, for $x = 0.2$ the concentration of electrons overtakes the concentration of hole for temperatures greater than 353 K and for $x = 0.5$–0.7, generation of electrons with increasing temperature may be expected, supported by the experimental decrease in resistivity. The observed decrease in n_c beyond typical temperatures for $x = 0.6$ and 0.7

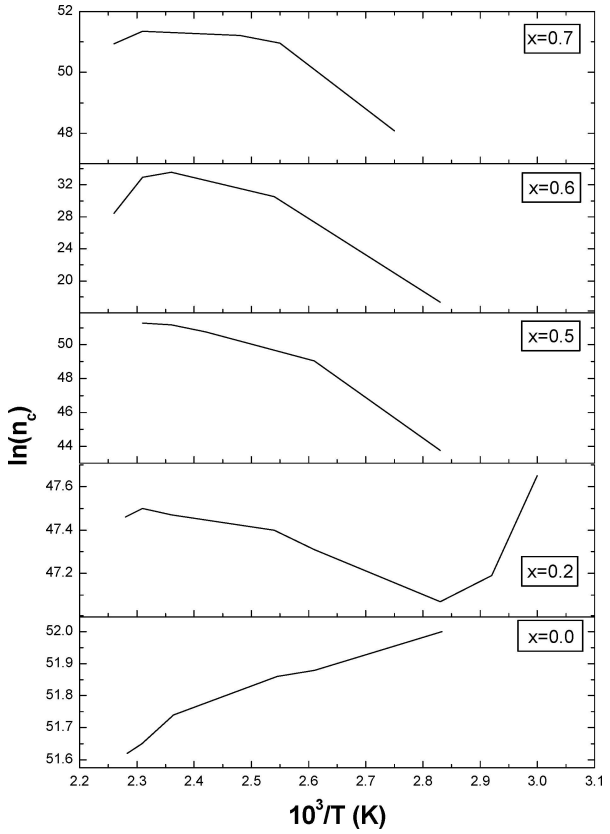

Figure 7 Variation of charge carrier concentration with reciprocal of temperature for $x = 0.0$, 0.2, 0.5, 0.6, and 0.7.

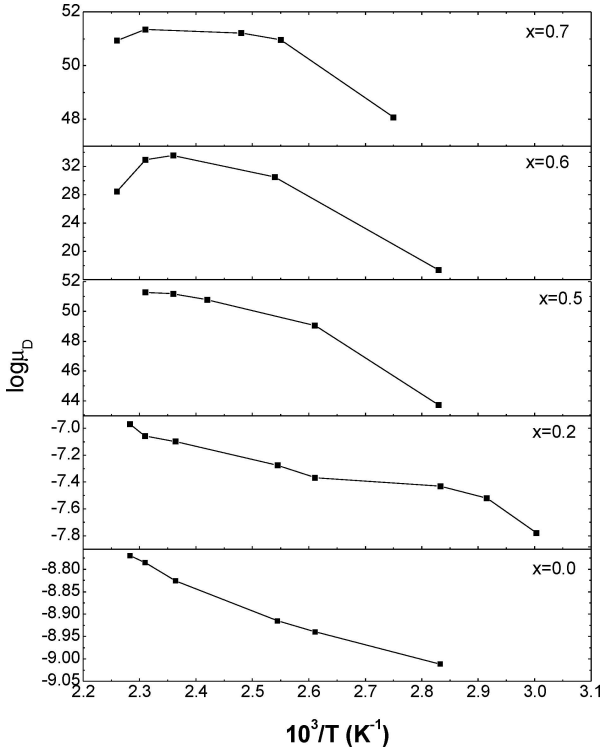

Figure 8 Thermal variation of mobility for $x = 0.0$, 0.2, 0.5, 0.6, and 0.7.

may be due to trapping of charge carriers at trapping centers.

The mobility (μ_D) of the charge carriers was calculated from the experimental values of the electrical resistivity (ρ_{dc}) and carrier concentration (n_c).

$$\mu_D = 1/\rho_{dc} \cdot n_c \cdot e$$

where e is electric charge of the carrier.

The thermal variations of the charge carrier mobility for the different compositions are shown in Fig. 8, as a plot of $\log\mu_D$ versus $10^3/T$. It is found that the mobility increases with increasing temperature for $x = 0.0$ and 0.2 while it is found to decrease with increasing temperature for $x = 0.5$. For the compositions with $x = 0.6$ and 0.7 it decreases up to a certain temperature and then starts increasing. The temperature from which μ_d found to increase is approximately 435 K and 392 K respectively for $x = 0.6$ and 0.7. These temperatures are in agreement with the corresponding Neel temperatures obtained experimentally from the thermal variation of the a.c. susceptibility [5] and the d.c. resistivity (Table III).

The magnitude of the mobility is found in the range of 10^{-7}–10^{-10} cm^2/V·sec ($T = 300$–450 K) for $x = 0.0$ and 0.2. This range is consistent with the mobility suggested in the literature [33] for holes (10^{-8} cm^2/V·sec). It is interesting to note that the compositions with $x = 0.5$, 0.6 and 0.7, in which it is found that the majority charge carriers are electrons from thermal variation of the Seebeck coefficient, mobility values are in the range of 10^{-12} cm^2/V·sec. This magnitude is much smaller that suggested for electrons (10^{-4} cm^2/V·sec). This supports the formation of small polarons.

The observed decrease in mobility with temperature for $x = 0.5$, 0.6 and 0.7 may be explained on the basis of two different phenomena:

(i) On increasing temperature lattice expansion take place, which hinders the hopping of the charge carriers.

(ii) On increasing temperature electrons interact with the lattice ions and distort the surroundings in such a way that the potential well thereby generated is deep enough to introduce localization.

3.4. I–V Characteristics measurements

Fig. 9 shows a typical current–voltage characteristic at two different temperatures (300 and 450 K) for compositions with $x = 0.0$, 0.2, 0.5, 0.6 and 0.7. It is evident from the figure that for the compositions with $x = 0.2$, 0.5, 0.6 and 0.7 an ohmic relationship is observed. The behaviour of the composition with $x = 0.0$ i.e. $Li_{0.5}Fe_{2.5}O_4$ is interesting, exhibiting a switching phenomenon. The current (I)–voltage (V) behaviour of any material at low electric field is linear (ohmic) due to the presence of thermally generated carriers. The observed non-ohmic I–V characteristics can be explained on the basis of the space-charge limited (SCL) current in the inhomogeneous solids which contain grain boundary layers. It is believed that in our case the observed nonlinearities in I–V characteristics are due to the contact resistance, if any, is negligible compared to that of basic material.

According to the band structure of solids, an insulator is characterized by a full valence band separated from an empty conduction band by a forbidden energy

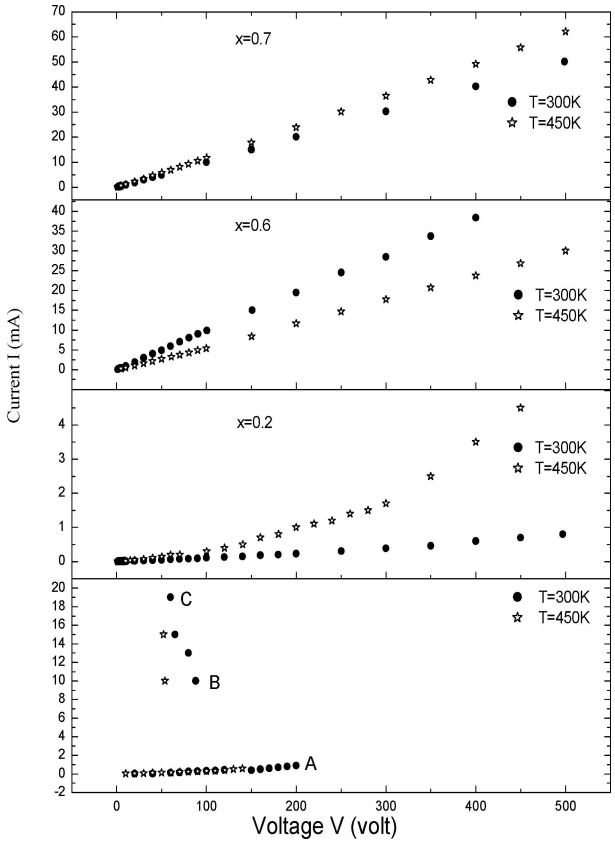

Figure 9 Current (I) versus voltage (V) relationship at 300 and 450 K for $x = 0.0$, 0.2, 0.6, and 0.7.

gap of a few electron volts. Evidently, conduction can not take place in either the filled or empty band unless additional carriers are introduced. Carriers may be generated inside the insulator or injected from the metal electrode or from metal insulator contacts [40] (bulk limited process). The simplest mechanism is the direct quantum mechanical tunneling of electrons from one metal electrode to the other.

When the injection into the conduction band or tunneling is not the rate limiting process for conduction in insulators, a space charge build up of the carriers in the valence band or at trapping centres (Fe^{4+}) may occur, which will oppose the applied voltage and impede the hole hopping. At low applied field, with a thermally generated free carrier density, Ohm's law is obeyed. When the injected carrier density is greater than the free carrier density the current becomes space charge limited. In insulators, as in semiconductors, a significant number of lattice defects capable of accepting one or more charge carriers may be present. These charge trapping centers must obviously modify the equilibrium concentration of the carriers and thus the SCL currents flow in an imperfect insulator.

From Fig. 9, we can see the nature of switching phenomenon in lithium ferrite sample. The deviation from Ohm's law becomes more prominent with the increase of voltage across the sample when the voltage is just over the value indicated by A in Fig. 9. For first time, the breakdown suddenly occurs and voltage falls to the value indicated by B (88 volts) denoted as first breakdown voltage. After this, current increases monotonously, from B to C. It can be seen that the first breakdown voltage decreases with increasing sample temperature (450 K). The switching current for the composition $x = 0.0$ is found to be 10 mA, which is in good agreement with the studies previously reported [41]. Above this switching voltage, the current increases monotonously accompanied with a decrease in voltage. Since the switching current is nearly the same for different temperatures, the explanation in terms of specific resistance and Joule self heating does not appear to be tenable. It is further observed that this cycle (path) is repetitive without any irregularities when tried for successive cycles. The properties of the sample were found not to be altered even when the cycle was repeated after two weeks. Therefore, the explanation of the switching behaviour for the present composition in terms of Joule self heating and specific resistance of the sample does not appear to be tenable.

4. Conclusions

Summing up the thermal variation of electrical properties of Mg^{2+} and Al^{3+} substituted $Li_{0.5}Fe_{2.5}O_4$ it is suggests that:

(i) Synthesized ferrite samples are electronic conductors, and for $x = 0.0$ and 0.2, conduction is due to holes while for $x = 0.5, 0.6$ and 0.7 it is due to electrons.

(ii) Thermal variation of mobility and activation energy values from d.c. resistivity measurements confirm formation of small polarons in the system.

(iii) Lithium ferrite ($x = 0.0$) exhibits a switching phenomenon, due to space charge limiting currents, while other compositions follow ohmic relationship.

Acknowledgement

One of the authors (KBM) is thankful to AICTE, New Delhi, for providing financial assistance in the form of career award for young teachers (2004).

References

1. D. RAVINDER and T. S. RAO, *Cryst. Res. Technol.* **25** (1990) 963.
2. D. RAVINDER, *Mat. Lett.* **40** (1999) 198.
3. A. A. SATTAR, A. H. WAFIK and H. M. EL-SAYED, *J. Mat. Sci*. **36** (2001) 4703.
4. N. REZLESCU, *Rev. Roum. Phys.* **15** (1970) 619.
5. R. MANJULA, V. R. K. MURTHY and J. SOBHANADRI, *J. Appl. Phys.* **59** (1986) 2929.
6. P. V. REDDY and T. S. RAO, *Phys. Stat. Sol.* (a) **92** (1985) 303.
7. G. J. BALDHA, K. G. SAIJA, K. B. MODI, H. H. JOSHI and R. G. KULKARNI, *Mat. Lett.* **53** (2002) 233.
8. K. B. MODI, J. D. GAJERA, M. C. CHHANTBAR, K. G. SAIJA, G. J. BALDHA and H. H. JOSHI, *ibid.* **57** (2003) 4049.
9. G. G. ROBERTS, in "Transfer and Storage of Energies by Molecules" (John-Wiley, New York, 1974) Vol. 4.
10. H. W. RUSSEL, *J. Am. Ceram. Soc.* **18** (1935).
11. B. GILLOT and F. JEMMALI, *Phys. Stat. Sol.* (a) **76** (1983) 601.
12. L. HEYNE, "Electrochemistry of Mixed ion Electroninc Conductors in Solid Electrolyte," edited by S. Geller (Springer-Verlag, New York, 1977) p. 169.
13. B. V. BHISE, M. G. PATIL, M. B. DONGARE, S. R. SAWANT and S. A. PATIL, *Ind. J. Pure Appl. Phys.* **30** (1992) 385.

14. H. B. LAL, B. K. VERMA and V. R. YADAV, *J. Mater. Sci.* **17** (1982) 3317.
15. V. R. YADAVA and H. B. LAL, *Canad. J. Phys.* **57** (1979) 1204.
16. A. B. NAIK, S. A. PATIL and J. I. PAWAR, *Ind. J. Pure Appl. Phys.* **27** (1989) 149.
17. S. A. PATIL, B. L. PATIL, S. R. SAWANT and R. N. PATIL, *ibid.* **31** (1993) 904.
18. B. V. BHISE, V. C. MAHAJAN, M. G. PATIL, S. D. LOTKE and S. A. PATIL, *ibid.* **33** (1995) 459.
19. A. A. GHANI, A. I. EATAH and A. A. MOHAMED, ICF-3, Japan (1980) p. 216.
20. A. P. KOMAR, *Bull. Acad. Sci. USSR Ser. Phys.* **18** (1954) 122.
21. K. R. KRISHNA MURTHY, Ph.D. Thesis, IIT Madras, India, 1975.
22. J. B. GOODENOUGH, *Mater. Res. Bull.* **8** (1973) 423.
23. M. W. ZEMANSKY, "Heat and Thermodynamics" (McGraw Hill, New York, 1968) p. 460.
24. A. J. BOSMAN and H. J. VAN DALL, *Adv. Phys.* **19** (1970) 1.
25. F. SEITZ, D. TURNBALL and H. EHRENREICH, *J. Appl Solid State Phys.* **21** (1968) 193.
26. I. G. AUSTIN and N. F. MOTT, *Adv. Phys.* **18** (1969) 41.
27. N. F. MOTT and E. A. DAVIS, "Phonons and Polarons in Electronics Processing in Non-Crystalline Materials" (Clarendon Press, Oxford, 1971).
28. N. REZLESCU and E. CUCIUREANU, *Phys. Stat. Sol.* **3** (1970) 873.
29. KUNAL B. MODI and H. H. JOSHI, *Ind. J. Phys.* **76A**(6) (2002) 543.
30. M. A. AHEMED, A. TAWFIK, M. K. EL NIMR and A. A. EL-HASEB, *J. Mat. Sci.* **10** (1991) 549.
31. A. B. DEVALE, Ph.D. Thesis, IISc Nagpur Uni., India, 1980.
32. L. G. VAN UITERT, *J. Chem. Phys.* **23** (1955) 1883.
33. M. A. AHMED, M. K. EL. NIMR, A. TAWFIK and A. M. EL. HASAB, *Phys. Stat. Sol.* (a) **123** (1991) 501.
34. S. S. BASHIKIRAV, A. B. LIBERMAN and V. V. PARFENOV, *Inorg. Mater.* **15** (1979) 404.
35. A. J. BOSMAN and C. CREVECOEUR, *J. Phys. Chem. Solids* **30** (1969) 1151.
36. *Idem.*, *Phys. Rev.* **144** (1966) 763.
37. R. R. HEIKES, in "Thermoelectricity," edited by R. R. Heikes and R. W. Ure (Wiley Interscience, NY, 1961) p. 45.
38. A. A. SAMOKHAVALOV and A. G. RUSTAMOV, *Soviet Phys.- Solid State* **6** (1953) 749.
39. F. J. MORIN, *Phys. Rev.* **93** (1953) 1195.
40. K. L. CHOPRA, "Thin Film Phenomena" (MacGraw Hill Book Company, New York, 1969).
41. T. YAMASHIRO, *Jap. J. Appl. Phys.* **12** (1973) 148.

Received 29 March
and accepted 6 December 2004